The Subluminous Supernova 2007qd: A Missing Link in Thermonuclear Deflagration

Colin M. M^{c}Clelland[1], Peter M. Garnavich[1], Lluís Galbany[2], Ramon Miquel[2], Ryan J. Foley[3,4], Bruce Bassett[5], Alexi V. Filippenko[6], J. Craig Wheeler[7], Ariel Goobar[8,9], Saurabh Jha[10], Donald P. Schneider[11], Joshua A. Frieman[12,13,14], Jozsef Vinko[15], Jesper Sollerman[16,17]

[1]Department of Physics, University of Notre Dame, Notre Dame, IN 46556

[2]Institut de Física d'Altes Energies, Universitat Autònoma de Barcelona, E-08193 Bellaterra (Barcelona) Spain

[3]Harvard-Smithsonian Center for Astrophysics, 60 Garden Street, Cambridge, MA 02138

[4]Clay Fellow

[5]Department of Mathematics and Applied Mathematics, University of Cape Town, Rondebosch 7701, South Africa

[6]Department of Astronomy, University of California, Berkeley, CA 94720-3411

[7]Department of Astronomy, McDonald Observatory, University of Texas, Austin, TX 78712

[8]Department of Physics, Stockholm University, Albanova University Center, SE-106 91 Stockholm, Sweden

[9]The Oskar Klein Centre for Cosmoparticle Physics, Department of Physics, AlbaNova, Stockholm University, SE-106 91 Stockholm, Sweden

[10]Department of Physics and Astronomy, Rutgers University, 136 Frelinghuysen Road, Piscataway, NJ 08854

[11]Department of Astronomy and Astrophysics, 525 Davey Laboratory, Pennsylvania State University, University Park, PA 16802

[12]Kavli Institute for Cosmological Physics, University of Chicago, 5640 South Ellise Avenue, Chicago, IL 60637

[13]Department of Astronomy and Astrophysics, University of Chicago, 5640 South Ellise Avenue, Chicago, IL 60637

[14]Center for Particle Astrophysics, Fermi National Accelerator Laboratory, P. O. Box 500, Batavia, IL 60510

[15]Department of Optics and Quantum Electronics, University of Szeged, Hungary

[16]Dark Cosmology Centre, Niels Bohr Institute, University of Copenhagen, Juliane Maries

Received _____; accepted _____

Vej 30, DK-2100 Copenhagen, Denmark

[17]Department of Astronomy, The Oskar Klein Centre, Stockholm University, 10691 Stockholm, Sweden

ABSTRACT

We present multi-band photometry and multi-epoch spectroscopy of the peculiar supernova 2007qd discovered by the SDSS-II Supernova Survey. The spectrum of SN 2007qd near maximum shows intermediate mass elements Si II, Ca II and S II, consistent with a Type Ia event, but with significantly slower photospheric expansion of only 2800 km s^{-1} as compared to over 10000 km s^{-1}. The spectral shapes evolve quickly and indicate the object cools rapidly. We find that the peak B-band magnitude of 2007qd is -15.4 ± 0.2 mag versus -19 mag for typical SN Ia, making it one of the most sub-luminous Type Ia supernovae ever observed. 2007qd appears to be a pure deflagration event with a brightness dimmer than other underluminous supernovae SN 2002cx and SN 2005hk yet stronger than the weak 2008ha explosion. We also compare 2007qd with conventional SN Ia alongside other SN types to ascertain the proper designation.

Subject headings: supernovae: individual (SN 2007qd) supernovae: photometry supernovae: spectroscopy

1. Introduction

For decades, Type Ia supernovae (SN Ia) have been interpreted as thermonuclear explosions through either accretion onto a degenerate white dwarf or via coalescence of two degenerate stars (for thorough reviews of these models, see Livio (2000)). Models that begin fusion subsonically and then turn into a detonation are best at matching observations of typical SN Ia. SN Ia show a range of energies and spectral charateristics, but the majority of events are extremely homogeneous when compared with other supernova types. The uniformity amongst SN Ia explosions have allowed their exploitation as a cosmic standard candles—the correlation between light curves' shape, peak luminosities (aka the Phillips relation) (Phillips 1993; Hamuy et al. 1996a) and colors (Riess et al. 1996; Guy et al. 2007) have enabled the precise measurement of cosmologically interesting distances. It is with these measurements, taken over a range of redshifts, that estimates of the Hubble parameter (H_0) and cosmic matter density have been refined (Hamuy et al. 1995; Riess et al. 1995; Garnavich et al. 1998; Freedman et al. 2001), and evidence for dark energy was revealed (Riess et al. 1998; Perlmutter et al. 1999).

The Sloan Digital Sky Survey-II (SDSS II) Supernova Survey was designed to further improve SN Ia as distance indicators (Frieman et al. 2008; Sako et al. 2008). Covering a 300 degree area with a rapid cadence, the survey discovered and spectroscopically confirmed roughly 500 SN Ia over a range of redshifts out to $z = 0.4$. Kessler et al. (2009a), Lampeitl et al. (2009) and Sollerman et al. (2009) used the first year of SDSS II data to constrain the dark energy equation of state parameter, (w), and analyzed the systematic errors limiting the cosmological measurements.

Identifying the progenitors of SN Ia and better understanding their explosion mechanism may improve their reliability as distance indicators. One approach is to study events that do not conform to the general SN Ia homogeneity in their spectra and/or

luminosity. Sub-classes of SN 1991T-like (Phillips et al. 1992; Filippenko 1992; Phillips 1993; Riess et al. 1996) and SN 1991bg-like (Filippenko et al. 1992a; Leibundgut et al. 1993; Turatto et al. 1996; Mazzali et al. 1997) events were quickly recognized as peculiar although much of the spectroscopic diversity is now known to be caused by a range of photospheric temperatures (Nugent et al. 1995).

Recently, additional sub-classes of SN Ia have been identified. For example, SN Ia 2002ic (Hamuy et al. 2003) and 2005gj (Prieto et al. 2005; Aldering et al. 2006) appear as luminous events that show hydrogen emission lines in their spectra. 02ic-like objects may be SN Ia interacting with dense circumstellar material, although a core-collapse scenario has also been proposed (Benetti et al. 2006). The supernova SN 2002cx (hereafter referred to as 02cx) was particularly peculiar. It showed a hot (91T-like) spectrum early-on, but it cooled quickly after maximum and its expansion velocities were well below typical for a SN Ia. 02cx deviated significantly from the Phillips relation by being subluminous for its light curve shape by $\tilde{1}.8$ mag in the B and V bands (Li et al. 2003; Jha et al. 2006). The well-observed SN 2005hk (05hk hereafter) was very similar to 02cx spectroscopically and was likewise subluminous by 0.6-1.0 mag in the optical (Phillips et al. 2007).

Jha et al. (2006) has identifed several other 02cx-like objects and has postulated that their extreme subluminosity consitutes a class of pure thermonuclear deflagrations. That is, the fusion front moving through the white dwarf fails to make the transition to supersonic burning (Branch et al. 2004) and is unable to generate the large amounts of radioactive nickel concurrent in typical SN Ia (Foley et al. 2009). The thermonuclear burning of carbon at moderate densities will create intermediate mass elements such as silicon, sulfur and calcium that dominate the spectrum. Though typical SN Ia experience this phase only briefly, Jha et al. (2006) reasoned that 02cx-like objects may burn completely via this mechanism.

So what characteristics separate delayed detonations from pure deflagrations? Simulations of pure deflagration events predict Rayleigh-Taylor instabilities will form clumps of radioactive nickel and mix unburned material towards the center (Reinecke et al. 2002; Gamezo et al. 2004; Travaglio et al. 2004; Schmidt & Niemeyer 2006). Late-time spectra of 02cx-like events show many iron and cobalt transitions broken up into thin spikes corresponding to the broad emissions in normal SN Ia (Jha et al. 2006; Kozma et al. 2005). Many narrow Fe II transitions persist for some time after the explosion, suggesting excitation by radioactive decay. Spectra of 05hk $\gtrsim$ 200 days past maximum have been analyzed for emission from "dredged-up" C I and O I, but their existence has at this time not been confirmed (Sahu et al. 2008).

An extremely subluminous transient, SN 2008ha (08ha hereafter) (Foley et al. 2009), appears to be an additional member of the 02cx class, although Valenti et al. (2009) have proposed that the extreme nature of 08ha (and other 02cx-likes) is better matched by the core-collapse of a massive star where most of the synthesized radioactive elements fall back to a black hole. With the discovery of Si II and S II in the early spectra of 08ha (Foley et al. 2010), that proposition becomes less likely.

Here, we report photometry and spectroscopy of SN 2007qd (07qd hereafter) discovered by the Sloan Digital Sky Survey II Supernova Survey. The observed properties of 07qd place it in the 02cx sub-class of supernovae, allowing us to test the competing models of their origin.

2. Observations

2.1. Photometry

07qd (Bassett et al. 2007) was discovered during the SDSS II Supernova Survey using the SDSS Camera on the 2.5 m telescope (Gunn et al. 1998, 2006) at Apache Point Observatory. The supernova was located at α =02h 09' 33.56", $\delta = -01^\circ$ 00' 02.2" (equinox 2000.0) (Bassett et al. 2007), amidst a spiral arm 10.6 kpc from the SBb/SBc host galaxy SDSS J020932.73-005959.8 centered at α =02h 09' 32.73" ,$\delta = -00^\circ$ 59' 59.80". The redshift of the host is $z = 0.043147 \pm 0.00004$, as measured from the SDSS galaxy redshift survey (York et al. 2000; Adelman-McCarthy et al. 2008). Figure 1 shows an image of the supernova and its location in its host galaxy. Foreground Local Galactic extinction in the direction of 07qd (Schlegel et al. 1998) is given in table 1 for the SDSS filters.

The photometry was calibrated in the standard SDSS *ugriz* photometric system (Fukugita et al. 1996; Smith et al. 2002). The flux from the supernova was estimated using the scene modeling technique (Holtzman et al. 2008) from individual calibrated images and without spatial resampling.

Figure 2 shows the SDSS-II light curves in the *ugriz* bands, listed in tabular form in Table 2. Bassett et al. (2007) noted that the spectrum of 07qd was similar to 05hk, so Figure 2 also features the 05hk light curves stretched to the observed frame of 07qd. In addition, the brightness of 05hk has been reduced by another 2.4 magnitudes to better match the peak flux of 07qd. The time of peak flux for 07qd is not well defined, but probably occured within a span of 2 days around MJD 54405 in the g band. Ignoring possible differences in dust extinction, 05hk is more luminous in all the SDSS bands and both rose and declined more slowly in the blue filters than 07qd. The light curve widths of the two supernovae are similar at near-infrared (SDSS i, z) wavelengths.

We compared the light curve of 07qd with additional SN to identify any similarity to Type Ic or II classes. We chose the fast-evolving 1994I (Yokoo et al. 1994; Richmond et al. 1996; Sauer et al. 2006), a well-observed prototype for SN Ic not accompanied by an X-ray flash or gamma ray burst, and 1999gi (Leonard et al. 2002), a Type IIP (plateau) SN that achieved a similar peak luminosity (described in detail in section 3.1). Figure 3 shows the general shapes of these light curves. Though the steep rise implied by 07qd's data proves similar to a SN IIP or SN Ic, the decline of 07qd and 05hk fail to represent the steep drop of 1994I or the extended plateau of 1999gi.

Figure 4 compares the color evolution of 07qd to that of 05hk, and reveals the former to be more blue near maximum. The colors of normal SN Ia are fairly well established (Phillips et al. 1999; Riess et al. 1996) and are used to estimate the reddening caused by dust in the host galaxy. However, the intrinsic colors of peculiar 02cx-like events are uncertain, making estimating host extinction problematic. But the blue color of 07qd compared to 05hk does suggest that dust extinction is not the major cause of the low luminosity of 07qd compared with 05hk.

2.2. Spectroscopy

Spectra of 07qd were obtained at four epochs utilizing three telescopes; A schedule of the observations is given in Table 3 and the resulting extracted and reduced spectra are detailed in figure 6, with 3-σ cosmic ray intrusions removed.

The Telescopio Nazionale Galileo (TNG) in the Canary Islands observed the 07qd at 3 days after maximum B (see section 3.1 for the determination of $B_{\max}$). The spectrum is a composite of three half-hour long exposures obtained with DOLORES (Device Optimized for LOw RESolution), a low resolution spectrograph and camera, equipped with a 2048

x 2048 E2V 4240 thinned back-illuminated, deep-depleted, Astro-BB coated CCD with a pixel size of 13.5 μm and with a field of view of 8.6' x 8.6' with a 0.252" px^{-1} scale, permanently installed at the Nasmyth B focus of the TNG. The spectra were observed with the low resolution blue grism (LR-B, dispersion 2.52 Å px^{-1}), covering the 3673-7401 Å range. A slit of 1.0" width, equal to the average seeing, was used for the observations and was aligned with the supernova and galaxy core.

The Hobby-Eberly Telescope (HET) at the McDonald Observatory in Texas produced spectra of 1200 s exposures utilizing the Marcario Low Resolution Spectrograph (LRS) (Hill et al. 1998) at 8 and 15 days past maximum. At the prime focus, the LRS employed a 0.235" px^{-1} plate scale with a 1" wide by 4' long slit and covered the $4075 - 9586$ Å range, though lower signal to noise ratios severely limit visibility past 8000 Å.

The W. M. Keck Observatory on Mauna Kea, Hawaii observed the SN at 10 days past maximum with the Low Resolution Imaging Spectrometer (LRIS) Oke et al. (1995) located at the Cassegrain focus of the Keck II telescope. The Keck measurement was able to cover bluer wavelengths than the other observations, spanning the $3073 - 8800$ Å range.

3. Analysis

3.1. Energetics

We began by applying the light curve fitters MLCS2k2 (Jha et al. 2007) and SALT2 (Guy et al. 2007) to the 07qd, 05hk, 02cx and 08ha data using the SNANA platform (Kessler et al. 2009b). The resulting fits were very poor quality with large reduced chi-squares ($\chi^2_{\rm d.o.f.} > 60$) and a clear inability for these algorithms, trained on normal events, to fit the colors and light curve shapes of these peculiar supernovae. One significant problem was lack of rise-time data on 07qd and 08ha, though a rise time of 10 ± 2 days can be inferred

for 07qd based on the non-detections in the SDSS-II data. This is a very short rise-time compared with typical SN Ia (Hayden et al. 2010). Combined with the odd colors, 07qd yielded light curve fits that were not useful for parameter estimation.

We decided to take a simple approach and estimate the B-band light curve stretch (Goldhaber et al. 2001) versus peak brightness for the peculiar events and more normal SN Ia. We used SNANA (Kessler et al. 2009b) to convert from $ugriz$ to the standard $UBVRI$ for SDSS-II SN Ia with $z < 0.12$. For 07qd we find a maximum absolute magnitude (after correcting only for Local, i.e. Milky Way Galactic extinction) of $M_B = -15.4 \pm 0.2$. We find the time of peak B brightness occurred on MJD 54405±2. Figure 5 compares 07qd's absolute magnitude and B-band stretch with 02cx, 05hk, 08ha and the normal SDSS-II SN (see Sako et al. (2008) for a list of these SN). The low-redshift set of SDSS-II contains a handful of 91bg-like events with stretch parameters ~ 0.8, but 07qd and 08ha have narrower light curves and are much fainter. There appears to be a sequence connecting the bright, peculiar events 05hk and 02cx to the extreme 08ha with the intermediate 07qd in Figure 5.

To examine the bolometric luminosities, a black-body was fit to the $ugriz$ SED as measured at B maximum. UV measurements shortward of u were not available for 07qd. 05hk and 08ha experienced severe photospheric line-blanketing for $\lambda < 3500$ Å (Phillips et al. 2007; Foley et al. 2009), which, along with our 10 day past maximum Keck spectrum, suggests 07qd's luminosity drops off sharply at that point. Using a Hubble constant of $H_0 = 73$ km s^{-1} Mpc^{-1} (Freedman et al. 2001; Riess et al. 2009) and integrating our SED (corrected for Milky Way extinction), a luminosity distance of 177 Mpc was computed and a peak quasi-bolometric luminosity was calculated to be $(4.44 \pm 0.5) \times 10^{41}$ erg s^{-1}. Using Arnett's rule (Arnett 1982; Arnett, Branch, Wheeler 1985) as applied by Stritzinger et al. (2006), we estimate the produced ^{56}Ni mass using

$$M_{\rm Ni} = L_{max}/L_{max}(1M_{\odot}) = \frac{4.44 \times 10^{41} {\rm erg\ s^{-1}}}{6.45 \times 10^{43} {\rm e}^{-t_R \lambda_{Ni}} + 1.45 \times 10^{43} {\rm e}^{-t_R \lambda_{Co}}},$$

where $\tau_{\rm Ni} = 1/\lambda_{\rm Ni}$ and $\tau_{\rm Co} = 1/\lambda_{\rm Co}$ are the exponential decay factors for ^{56}Ni and ^{56}Co, respectively. Thus, for $t_R = 10 \pm 2$ d, we estimate $M_{\rm Ni} = 0.013 \pm 0.002\, M_{\odot}$, which is an order of magnitude larger than 08ha's $(3.0 \pm 0.9) \times 10^{-3}\, M_{\odot}$ (Foley et al. 2009) but still much smaller than 05hk's 0.22 $M_{\odot}$ (Phillips et al. 2007). Here, we assume the ratio between bolometric and radioactivity luminosities is unity. Howell et al. (2009) argues the nickel mass may in fact be smaller by a factor of $1/(1.2 \pm 0.1)$ if the metallicity around the SN is significantly larger than solar, but upon measuring the host galaxy's abundance (see section 3.2.3), we find this case to be unlikely. This ejecta mass, coupled with the photospheric velocity measured at 3 days past maximum (see section 3.2.1), predicts a kinetic energy of roughly 08ha's 10^{50} ergs, less than the estimated binding energy of 10^{51} ergs for a 1.4 $M_{\odot}$ white dwarf.

3.2. Spectroscopy

We used SYNOW (Fisher et al. 1997; Fisher 2000), a parameterized supernova spectrum synthesis code, to fit our spectra to profiles of various ions at specific velocities, excitation temperatures and opacities. These ions are simulated in an expanding photosphere of a chosen black-body temperature, and the resulting spectra can be extracted and compared with data. Due to the high number of parameters used in SYNOW (3 for the photosphere plus 7 for each ion species), this process can be arduous and extremely resource-intensive for precise results (Nugent et al. 2008). We systematically fit our spectra with ions commonly seen in SN Ia at similar epochs (Fe II, Co II, Si II, etc.), and attempted to simulate hydrogen and helium to rule out the possibility of a Type II or Ibc SN. The photospheric velocity was fixed at each epoch by the best fit for the Fe II lines, and

subsequent elements were fit either residing in that photosphere or at detached velocities. After confirming the presence or absence of these species, we attempted to fit elements uncommon to normal SN Ia in order to fit any remaining line profiles.

We also attempted to use Na I D host and interstellar absorption to measure dust extinction though the procedures of Munari & Zwitter (1997). The signal to noise of our spectra, combined with the numerous velocity features and transitions scattered over the continuum created too much uncertainty in these equivalent widths to fix an extinction value.

3.2.1. +3 Days Spectrum

Figure 7 and Table 4 show the results of our SYNOW fit to the spectrum 3 days past maximum. We found, from the Fe II fitting, a photospheric velocity of 2800 km s^{-1} which is extraordinarily low. Typical SN Ia photospheric velocities at the epoch are often in excess of 10,000 km s^{-1} (Pskovskii 1977; Branch et al. 1981). The low velocites found for most of the regions makes it highly unlikely that the strong feature at 6300 Å is from hydrogen or helium either in the photosphere or detached. The best fit to the 6300Å absorption was Si II as Fe II was constrained in fitting the $\tilde{6}$100 Å,$\tilde{6}$200 Å, $\tilde{6}$400 Å transitions as well as others further in the bluer regions. Also prominent in the 6100 Å region is a broad primary O I line. The secondary signatures of this O I are slightly seen at $\tilde{5}$300 Å, but masked at $\tilde{6}$400 Å due to the strong Si II edge. C III was also used to help Co II shape the area around $\tilde{4}$600 Å and C II was necessary for an absorption feature at $\tilde{6}$550 Å, albeit with a larger excitation temperature which subdues the effects of secondary lines. The presence of ions, such as Si IV, and the absence of others, such as C I, run contradictory to models for SN Ia spectra in Hatano et al. (1999). It should also be noted that O II, Ni II and Co III, predicted by those models, may be added to the fit with large optical depths but affecting

it little.

3.2.2. +10 Days Spectrum

The fit in Figure 8 is derived from parameters used to fit 02cx at 12 days past maximum (Branch et al. 2004), except the velocities and black-body temperature have been reduced to accommodate 07qd's unique nature. This fit was chosen due to its consistency in representing 08ha, 02cx and 05hk at similar epochs, as is seen in figure 10. The similarity is especially apparent with 08ha, which shares most absorption features with 07qd. The relative shift between these two spectra was measured to be an offset of roughly 800 km s^{-1} from 08ha's photosphere velocity of 2000 km s^{-1}, which corresponds the best-fit SYNOW photospheric velocity of 07qd, estimated to be 2800 km s^{-1} with a black-body temperature of 8000 K. Although Foley et al. (2009) found an excellent match with a SYNOW fit to a 14-day spectrum of 08ha with a photospheric velocity of only 600 km s^{-1}, we attempted one with the estimated velocity.

Much of the continuum is dominated by narrow Fe II lines, with Co II playing a large role below 5000 Å as well, consistent to most iron-core SN (Harkness et al. 1991). The modified SYNOW fit also continues to include a prominent Si II feature at 6300 Å neccessitated by Fe II's inability to fit it without losing other features. This Si II resides within the photosphere and has a maximum velocity imposed at 3800 km s^{-1} in exactly the same manner as Fe II and Co II, so no new treatment is necessary. The addition of Si II also enhances the spectrum at $\tilde{4}$100 Å but less so at $\tilde{3}$850 Å and $\tilde{5}$025 Å. The carbon and vanadium measured at 3 days past maximum are not prominent at any ionization level nor necessary, though their existence cannot be ruled out, partly to line blocking by the dominant Fe II lines (Baron, Lentz, Hauschildt 2003). The Cr-II in Branch et al. (2004)'s fit of 02cx is also not necessary, as there is insufficient data to examine regions below 3750

Å at this and later epochs.

The signal-to-noise of the data appears to be lower than it actually is, attributing to the low-velocity nature of this particular photosphere. Much of the absorption blending in the regions blueward of 4500 Å prove difficult to fit with SYNOW models, especially where P Cygni profiles are no longer apparent.

Hα and helium ions were tested in SYNOW fits, though no match could be found. We expect and observe galactic Hα emission at 6563 Å, though just blueward of this feature we observe a small absorption that we are unable to identify. It is very unlikely this is a P Cygni Hα signature as there is insufficient velocity to generate a discrepancy between the emission and absorption. However, features such as the structure at $\tilde{6}$550 Å are attributable to a combination of sky lines and the supernova spectra's unfortunate proximity to the host galaxy's Hα emission. It is unclear at this time what the trough at 6750 Å is; very few ions are capable to modeling it without severely affecting the fit elsewhere, but detached F I is a possibility if the F II suspected at 3 days is no longer present. He I was of particular interest in Valenti et al. (2009)'s SYNOW fit to 08ha's 13 day spectrum, but the Na I D line dominates over the predicted He I line. At 10 days past maximum, all other He I features fail to match the spectrum. Possible ions include Sc II (for the absorption at 5450 Å), C II (for the small 6450 Åtrough or the trough preceding the "Hα" feature), and Ti II for its general blending in the blue portions of the spectrum. The greatly different photospheric velocities apparent between 07qd and 05hk are examined along with 02cx and 08ha in figure 9, suggesting a relation to the luminosities in these peculiar cases.

3.2.3. Spectral Evolution and Similarity to other SN Ia

Using these SYNOW fits to the individual epochs, the spectral evolution of 07qd given in figure 6 now provides a detailed picture of a developing photosphere. Examining the $\tilde{4}550$ and $\tilde{5}200$ Å edge-features present at 3 days but absent at 10 days, Fe III has either greatly reduced it's opacity or recombined into Fe II, which has increased in influence. Na I and S II have decreased in intensity, but remain crucial to the region between 5000 and 6000 Å.

The Si II feature endures through two weeks past maximum, but its impact has lessened and has relatively equal absorption magnitude to that of Fe II by 13 days. This strength and persistence of the Si II line clearly distinguishes 07qd from the Shallow-Silicon group mentioned in Branch et al. (2009). Much of the spectra in the blue was not measured in subsequent epochs, though extended red wavelengths are given, revealing probable O I and O II signatures. It is apparent, however, that the first week's spectroscopic data beyond 8000 Å does not discern a rising or falling Ca II IR feature, though the Ca II H&K UV lines persist. Consequently, elements such as V II, F II and Al I are no longer measurable without the blue wavelengths beyond 4000 Å. Black-body temperatures have fallen to 8000 K at 8 days past maximum and 6000 K at 13 days, further intensifying the influence of Fe II profiles over the continuum. It remains to be seen whether the remaining unfit line profiles can be remedied with more exotic ions.

Figure 10 shows the spectra of four 02cx-like SN Ia compared at similar epochs. 07qd clearly bears the strongest resemblance to 08ha, as very few features differ. 02cx and 05hk present much faster photospheres than 07qd and 08ha, and are likewise shifted towards the blue. The faster photosphere and higher excitation temperatures used in Branch et al. (2004)'s SYNOW fit of 02cx also broadens many of the Fe II features, effectively masking the primary Si II absorption. Other major velocity features, however, remain consistent. It should be noted, however, that SYNOW's highly parameterized fitting routine is subject to

large degrees of freedom. Conclusive simulations of Si II and S II in 07qd may be obtained in the future via other sophisticated spectral simulations (Lucy 1999; Mazzali 2000).

In order to independently identify these intermediate metals outside of simulations, we directly compared 07qd's spectra with other confirmed SN Ia. Of special interest is 07qd's spectral relation to SN 2004eo (hereafter called 04eo). Similar to the prototypical SN 1992A (Hamuy et al. 1996c), 04eo is characterized as a fast-declining SN Ia with slow photospheric velocities. However, it retains an absolute B maximum of -19.08 (within the range of "normal" SN Ia) and still fits the Phillips Relation. Spectroscopically, 04eo contains strong Si II and S II line strengths in its spectra, also typical of SN Ia (Pastorello et al. 2007). When 07qd's spectra are blueshifted to coincide with 04eo's photospheric velocity, many common features become apparent, especially the Si II and S II. Figure 11 shows a normalized comparison between early spectra from 07qd and 04eo that highlights both the presence and the relative strength of these intermediate metals.

3.3. Host Galaxy

The host galaxy in figure 1 shows a prominent bar and two major spiral arms. The low inclination allows minor spiral arms to be distinguishable, one of which contains 07qd's location. The classifications of SBb or SBc suggest star formation, but 02cx-like SN Ia appear to span a wide variety of galactic morphologies (Foley et al. 2009; Valenti et al. 2009). The Keck II spectrum also included the host galaxy's core in the slit aperture, allowing a basic measurement of oxygen abundance. We used both the optimized method recommended in Kewley & Dopita (2002) and the [NII]/[OII] diagnostic to arrive at an oxygen abundance in the host galaxy of $12 + \log(\mathrm{O/H}) = 8.79 \pm 0.03$. This is equivalent to the sun's $8.76 \pm .07$ oxygen abundance (Caffau et al. 2008) but it exceeds that of 08ha's host, measured to be 8.16 ± 0.15 by Foley et al. (2009) using N2 and O3N2 diagnostics

(see Pettini & Pagel (2004)). The host galaxy's oxygen abundance also places weight on the nickel mass estimated in section 3.1, as our calculated abundance does not deviate from solar enough to warrant an efficiency correction (Howell et al. 2009). The statistics presented by Boissier & Prantzos (2009) suggest a slight proclivity towards core-collapse SN over SN Ia at these abundances, but offer no conclusive argument on typing.

4. Discussion

The striking similarity of 07qd's 10 day old spectrum to that of 08ha suggest that they are indeed similar explosions. Since 07qd is also spectroscopically linked to 05hk and 02cx, these four peculiar events range in peak brightness by four magnitudes, but constitute a single spectral class.

Valenti et al. (2009) argued that 08ha and possibly other 02cx-like objects were actually core-collapse SN; the underluminosity was the result of either the direct-to-black hole collapse of a $\gtrsim 30\ M_{\odot}$ star or electron capture in the core of a 7-8 $M_{\odot}$ star. However, 07qd showing the clear presence of intermediate mass elements (notably Si II 6355 and S II 5968, 6359) shows mixing during a thermonuclear runaway and not a core-collapse Type Ib or Ic (see Filippenko (1997) for a review of SN spectroscopic classification). Evidence of these intermediate metals' presence apart from SYNOW fits has been seen upon comparison to 92A-like SN Ia, and misidentification of these features is furthermore unlikely.

The presence of these metals mirror the findings of Foley et al. (2010); although it is possible for a SN Ibc to show traces of Si II (Valenti et al. 2008) or hypernova associated S II (Nomoto et al. 2000; Brown et al. 2007), it is highly unlikely that both are seen in such an event. Additionally, the light curve of 07qd, though displaying a sharp rise that is unusual for a typical SN Ia, does not show the fast decline typical of a SN Ic or the plateau feature of

a SN IIP that achieves similar peak luminosity. The energy released by 07qd is substantially lower than normal SN Ia, but the predicted nickel mass serves as an intermediate example between 08ha and 05hk, further linking the two groups. It is concerning, under traditional models, that the extremely low ejecta mass and the photospheric velocities under 3000 km s^{-1} prove difficult to disrupt a 1.4 $M_{\odot}$ white dwarf (Foley et al. 2009), suggesting energy input differing from Arnett's Rule or other than ^{56}Ni during the explosion.

When compared with other 02cx-like SN, 07qd's spectra mirror that of 08ha and suggest the Si II 6355 feature in the latter. These comparisons also suggest that strong Si II is possible in 02cx and 05hk, though "disguised" by Fe II blending due to the higher velocities. The fast decline of 07qd suggest that these intermediate metals are only visible for a brief time and become masked by Fe II or recombine as the photosphere slows and cools. The presence of carbon and oxygen ions in the photosphere echoes the results of deflagration models including Gamezo et al. (2004), suggesting the presence of unburned white dwarf material and supporting that this class stems from such a progenitor. Extremely low expansion velocities, however, eliminate 07qd as a candidate for the ".Ia" model for AM Canum Venaticorum white dwarfs (Bildsten et al. 2007).

The low velocities and energies present 08ha and 07qd enable the analysis of many aspects of 02cx-like SN, otherwise hidden by the Fe II blending concurrent with 05hk and 02cx. Furthermore, the transitions revealed at these optical depths may shed light on deflagration explosion mechanisms. Though the velocities and energies of these two subgroups are different, they remain generally similar with regard to other SN, and together they constitute a common group of peculiar SN Ia.

Funding for the SDSS and SDSS-II has been provided by the Alfred P. Sloan Foundation, the Participating Institutions, the National Science Foundation, the U.S. Department of Energy, the National Aeronautics and Space Administration, the Japanese

Monbukagakusho, the Max Planck Society, and the Higher Education Funding Council for England. The SDSS Web Site is http://www.sdss.org/.

The SDSS is managed by the Astrophysical Research Consortium for the Participating Institutions. The Participating Institutions are the American Museum of Natural History, Astrophysical Institute Potsdam, University of Basel, University of Cambridge, Case Western Reserve University, University of Chicago, Drexel University, Fermilab, the Institute for Advanced Study, the Japan Participation Group, Johns Hopkins University, the Joint Institute for Nuclear Astrophysics, the Kavli Institute for Particle Astrophysics and Cosmology, the Korean Scientist Group, the Chinese Academy of Sciences (LAMOST), Los Alamos National Laboratory, the Max-Planck-Institute for Astronomy (MPIA), the Max-Planck-Institute for Astrophysics (MPA), New Mexico State University, Ohio State University, University of Pittsburgh, University of Portsmouth, Princeton University, the United States Naval Observatory, and the University of Washington.

We would also like to thank the National Science Foundation, the University of Notre Dame, Brian Hayden, Joe Gallagher and Weidong Li for discussions and their help in the production of this paper. We'd also like to thank Jerod Parrent and the Online Supernova Spectrum Archive (SUSPECT) and David Jeffery along with the SUSPEND database.

REFERENCES

Adelman-McCarthy, J. K., et al. 2008, ApJ, Suppl. 175, 297

Aldering, G., et al. 2006, ApJ, 650, 510

Arnett, W. D. 1982, ApJ, 253, 785

Arnett, W. D., Branch, D., Wheeler, J. C. 1985, Nature, 314, 337

Baron, E., Lentz, E. J., Hauschildt, P. H. 2003, ApJ, 588, L29

Bassett, B., et al. 2007, CBET, 1137

Benetti, S., et al. 2005, ApJ, 623, 1011

Benetti, S., Cappellaro, E., Turatto, M., Taubenberger, S., Harutyunyan, A., & Valenti, S. 2006, ApJ, 653, L129

Bildsten, L., Shen, K. J., Weinberg, N. N., & Nelemans, G. 2007, ApJ, 662, L95

Boissier, S., & Prantzos, N. 2009, A&A, 503, 137

Branch, D. 1981, ApJ, 248, 1076

Branch, D., Baron, E., Thomas, R. C., Kasen, D., Li, W., Filippenko, A. 2004, PASP, 116, 903

Branch, D., Dang, L. C., Baron, E. 2009, PASP, in production

Brown, G. E., Lee, C.-H., & Moreno Méndez, E. 2007, ApJ, 671, L41

Caffau, E., Ludwig, H.-G., Steffen, M., Ayres, T. R., Bonifacio, P., Cayrel, R., Freytag, B., & Plez, B. 2008, A&A, 488, 1031

Cardelli, J. A., Clayton, G. C., & Mathis, J. S. 1989, ApJ, 345, 245

Chornock, R., Filippenko, A. V., Branch, D., Foley, R. J., Jha, S., & Li, W. 2006, PASP, 118, 722

Danziger, I. J., Kjär, K., eds. 1991, Supernova 1987A and Other Supernovae, Conf. Proc. No. 37. Garching: Eur. Southern Obs.

Filippenko, A. V., Richmond, M. W., Branch, D., Gaskell, C. M., Herbst, W., et al. 1992, AJ, 104, 1543

Filippenko, A. V., Richmond, M. W., Matheson, T., Shields, J. C., Burdridge, E. M., et al. 1992, ApJ, 384, L15

Filippenko, A. V. 1992, ApJ, Lett. 384, L37

Filippenko, A. V. 1997, ARA&A, 35, 309

Fisher, A., Branch, D., Nugent, P., & Baron, E. 1997, ApJ, 481, L89

Fisher, A. 2000, PhD. Thesis, University of Oklahoma

Foley, R. J., et al. 2009, astro-ph/0902.2794

Foley, R. J., Brown, P. J., Rest, A., Challis, P. J., Kirshner, R. P., & Wood-Vasey, W. M. 2010, ApJ, 708, L61

Freedman, W. L., et al. 2001, ApJ, 553, 47

Frieman, J. A., et al. 2008, AJ, 135, 338

Fukugita, M., et al. 1996, AJ, 111, 1748

Gamezo, V. N., Khokhlov, A. M., & Oran, E. S. 2004, Cosmic explosions in three dimensions, 121

Garnavich, P. M., et al. 1998, ApJ, 493, L53

Goldhaber, G., et al. 2001, ApJ, 558, 359

Gunn, J. E., et al. 1998, AJ, 116, 3040

Gunn, J. E., et al. 2006, AJ, 131, 2332

Guy, J., et al. 2007, A&A466, 11

Hamuy, M., Phillips, M. M., Maza, J., Suntzeff, N. B., Schommer, R. A., Avilés, R. 1995, AJ, 109, 1

Hamuy, M., Phillips, M. M., Schommer, R. A., Suntzeff, N. B., Maza, J., Avilés, R., et al. 1996a, AJ, 112, 2391

Hamuy, M., Phillips, M. M., Suntzeff, N. B., Schommer, R. A., Maza, J., et al. 1996b, AJ, 112, 2398

Hamuy, M., Phillips, M. M., Suntzeff, N. B., Schommer, R. A., Maza, J., Smith, R. C., Lira, P., & Aviles, R. 1996, AJ, 112, 2438

Hamuy, M. et al. 2003, Nature, 424, 651

Harkness, R. P. 1991, See Danziger & Kjär 1991

Hatano, K., Branch, D., Fisher, A., Millard, J., & Baron, E. 1999, ApJS, 121, 233

Hayden, B. T., et al. 2010, arXiv:1001.3428

Hill, G. J., et al. 1998, SPIE Conf., Kona, March 1998, 3355, p424

Holtzman, J. A., et al. 2008, AJ, 136, 2306

Howell, D. A., et al. 2009, ApJ, 691, 661

Jha, S., et al. 2004, AJ, 132, 189

Jha, S., Riess, A. G., Kirshner, R. P. 2007, ApJ, 659, 122

Kasen, D. 2006, ApJ, 649, 939

Kewley, L. J., & Dopita, M. A. 2002, ApJS, 142, 35

Kessler, R., et al. 2009, ApJS, 185, 32

Kessler, R., et al. 2009, PASP, 121, 1028

Kozma, C., Fransson, C., Hillebrandt, W., Travaglio, C., Sollerman, J., Reinecke, M., Röpke, F. K., & Spyromilio, J. 2005, A&A, 437, 983

Lampeitl, H., et al. 2009, MNRAS, 1782

Leibundgut, B., Kirshner, R. P., Phillips, M. M., Wells, L. A., Suntzeff, N. B., et al. 1993, AJ, 105, 301

Leonard, D. C., et al. 2002, AJ, 124, 2490

Li, W., et al. 2003, PASP, 115, 453

Livio, M. 2000, Type Ia Supernovae, Theory and Cosmology, 33

Lucy, L. B. 1999, A&A, 345, 211

Lupton, R. H., Gunn, J. E., & Szalay, A. S. 1999, AJ, 118, 1406

Mazzali, P. A., Chugai, N. N., Turatto, M., Lucy, L. B., Danziger, I. J., et al. 1997, MNRAS, 284, 151

Mazzali, P. A. 2000, A&A, 363, 705

Munari, U., & Zwitter, T. 1997, A&A, 318, 269

Nomoto, K., et al. 2000, Gamma-ray Bursts, 5th Huntsville Symposium, 526, 622

Nugent, P., Phillips, M., Baron, E., Branch, D., & Hauschildt, P. 1995, ApJ, 455, L147

Nugent, P., Thomas, R., & Aldering, G. 2008, Journal of Physics Conference Series, 125, 012011

Oke, J. B., et al. 1995, PASP, 107, 375

Pastorello, A., et al. 2007, MNRAS, 377, 1531

Perlmutter, S., et al. 1999, ApJ, 517, 565

Pettini, M., & Pagel, B. E. J. 2004, MNRAS, 348, L59

Phillips, M. M., et al. 1992, AJ, 103, 1632

Phillips, M. M. 1993, ApJ, 413, L105

Phillips, M. M., et al. 1999, AJ, 118, 1766

Phillips, M. M., et al. 2007, PASP, 119, 360

Pinto, P. A., & Eastman, R. G. 2000, ApJ, 530, 757

Prieto, J., Garnavich, P., Depoy, D., Marshall, J., Eastman, J., & Frank, S. 2005, Central Bureau Electronic Telegrams, 302, 1

Pskovskii, Yu. P. 1977, Sov. Astron. 21, 675

Reinecke, M., Hillebrandt, W., & Niemeyer, J. C. 2002, A&A, 391, 1167

Richmond, M. W., et al. 1996, AJ, 111, 327

Riess, A. G., Press, W. H., Kirshner, R. P. 1995, ApJ, 438, L17

Riess, A. G., Press, W. H., Kirshner, R. P. 1996, ApJ, 473, 88

Riess, A. G., et al. 1998, AJ, 116, 1009

Riess, A. G., et al. 2009, astro-ph/0905.0695

Sahu, D. K., et al. 2008, ApJ, 680, 580

Sako, M., et al. 2008, AJ, 135, 348

Sauer, D. N., Mazzali, P. A., Deng, J., Valenti, S., Nomoto, K., & Filippenko, A. V. 2006, MNRAS, 369, 1939

Schlegel, D. J., Finkbeiner, D. P., & Davis, M. 1998, ApJ, 500, 525

Schmidt, W., & Niemeyer, J. C. 2006, A&A, 446, 627

Smith, J. A., et al. 2002, AJ, 123, 2121

Sollerman, J., et al. 2009, ApJ, 703, 1374

Stritzinger, M., et al. 2006, A&A, 450, 241

Travaglio, C., Hillebrandt, W., Reinecke, M., & Thielemann, F.-K. 2004, A&A, 425, 1029

Turatto, M., Benetti, S., Cappellaro, E., Danziger, I. J., Della Valle, M., et al. 1996, MNRAS, 283, 1

Valenti, S., et al. 2008, ApJ, 673, L155

Valenti, S., et al. 2009, Nature, 459, 674

Woosley, S. E., Kasen, D., Blinnikov, S., & Sorokina, E. 2007, ApJ, 662, 487

Yokoo, T., Arimoto, J., Matsumoto, K., Takahashi, A., & Sadakane, K. 1994, PASJ, 46, L191

York, D. G., et al. 2000, AJ, 120, 1579

This manuscript was prepared with the AAS LaTeX macros v5.2.

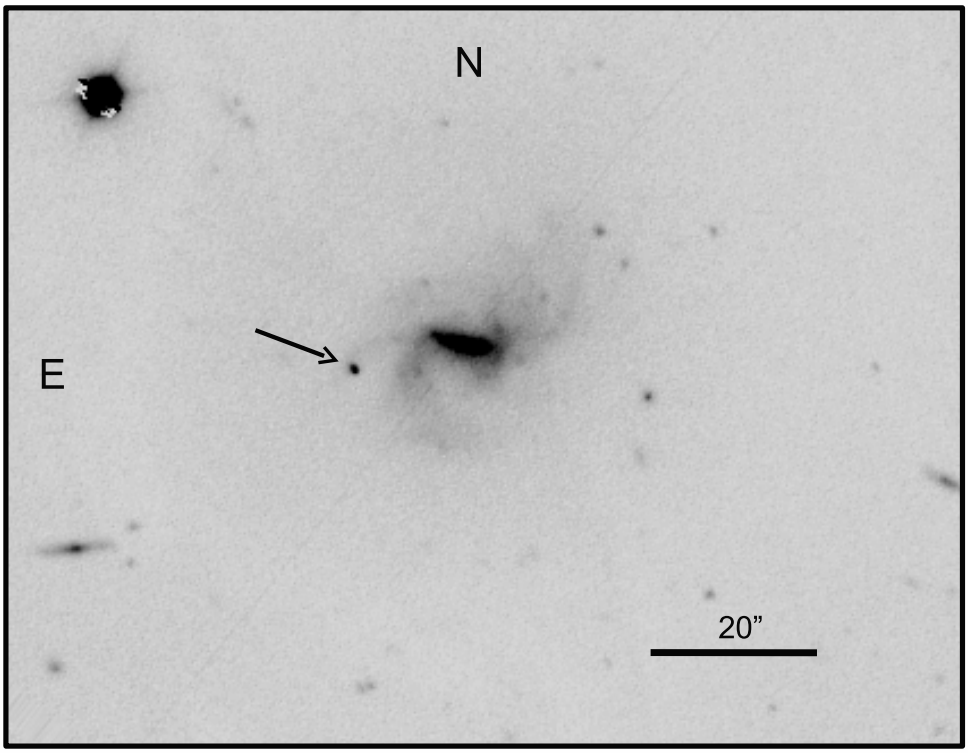

Fig. 1.— Image of 07qd (denoted by arrow) relative to its host galaxy in a 1’ 45” by 1’ 20” window. The 90-second unfiltered exposure was taken on MJD 54409.08 with the TNG telescope.

Table 1. Local (Milky Way) Galactic Extinction

Filter	A_λ [mag]
u	0.178
g	0.131
r	0.095
i	0.072
z	0.051

Table 2. Observed SDSS photometry for 07qd (SN 20208), converted into flux densities. [a,b]

MJD	u [μJy]	g	r	i	z
54346.41	-0.010 ± 2.726	1.620 ± 1.230	0.880 ± 1.235	-0.730 ± 1.281	-1.100 ± 3.851
54348.41	-1.780 ± 1.614	0.610 ± 0.648	1.520 ± 0.698	0.200 ± 1.019	1.600 ± 3.929
54355.42	1.500 ± 2.146	-0.470 ± 0.530	0.410 ± 1.111	-0.370 ± 1.813	5.870 ± 5.868
54358.37	4.310 ± 1.878	0.870 ± 0.530	-0.000 ± 0.707	-1.480 ± 1.159	-1.940 ± 4.186
54365.40	0.000 ± 0.971	-0.180 ± 0.315	0.000 ± 0.496	-1.500 ± 0.719	-1.470 ± 3.225
54381.42	1.400 ± 1.165	0.010 ± 0.362	-0.090 ± 0.590	-0.340 ± 0.790	-4.300 ± 3.010
54384.43	1.550 ± 1.396	0.130 ± 0.393	-0.580 ± 0.557	-2.860 ± 0.817	-5.780 ± 3.438
54386.41	0.260 ± 1.478	0.080 ± 0.489	0.230 ± 0.634	0.670 ± 0.846	-1.960 ± 4.057
54388.42	0.240 ± 1.431	0.270 ± 0.399	0.060 ± 0.587	-0.250 ± 0.779	2.090 ± 3.177
54392.42	-0.840 ± 1.554	-0.420 ± 0.556	1.160 ± 0.837	0.120 ± 1.228	-1.630 ± 4.251
54393.42	2.100 ± 1.731	-0.020 ± 0.564	-0.670 ± 0.546	-0.050 ± 0.850	3.650 ± 4.373
54396.29	-7.950 ± 7.556	-2.870 ± 3.713	0.720 ± 2.329	-	-3.160 ± 7.688
54405.39	13.620 ± 2.416	19.170 ± 1.007	16.510 ± 0.990	15.750 ± 1.281	7.640 ± 4.463
54406.33	6.930 ± 1.466	17.310 ± 0.638	17.080 ± 0.709	15.930 ± 0.912	17.020 ± 2.989
54412.35	2.470 ± 1.702	9.760 ± 0.514	15.720 ± 0.899	13.850 ± 1.204	15.080 ± 4.166
54416.32	0.920 ± 1.072	6.350 ± 0.388	14.140 ± 0.574	13.620 ± 0.769	17.010 ± 3.035
54421.33	3.480 ± 1.736	5.250 ± 0.502	13.290 ± 0.797	11.980 ± 1.110	12.360 ± 4.757
54423.31	1.060 ± 1.924	4.200 ± 0.829	12.460 ± 1.058	13.620 ± 1.197	19.620 ± 3.800
54433.33	-	5.430 ± 1.501	8.780 ± 2.494	9.740 ± 2.832	5.980 ± 6.150

[a]Not corrected for galactic extinction.

[b]Data associated with poor seeing have been omitted from this list.

Table 3. Spectra observation schedule

Telescope	Date	Time [UT]	Days since B_{max}	Exposure [s]	Range [Å]
TNG	5 Nov, 2007	02:06:10	+3	3 × 1800	3673-7401
HET	10 Nov, 2007	04:23:12	+8	1200	4075-9586
Keck	12 Nov, 2007	12:39:01	+10	1500	3073-8800
HET	17 Nov, 2007	03:58:29	+15	1200	4074-9586

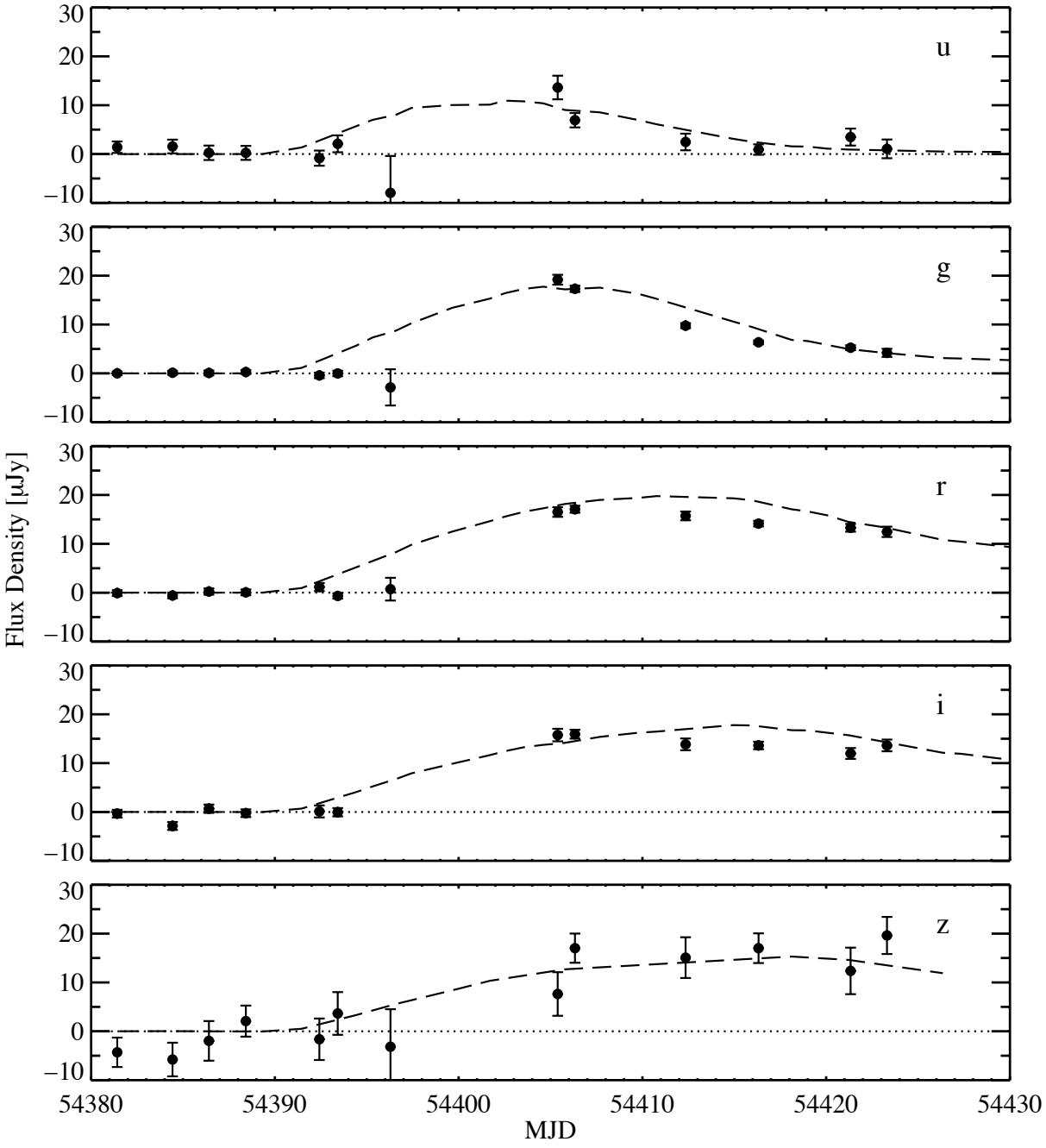

Fig. 2.— SDSS apparent light curves of 07qd given in flux units. The dashed line represents 05hk's combined SDSS and CSP light curve data in 07qd's rest frame, positioned over 07qd's maximum, and artificially shown 2.4 magnitudes fainter for better comparison of their shapes. Neither light curve has been corrected for galactic extinction.

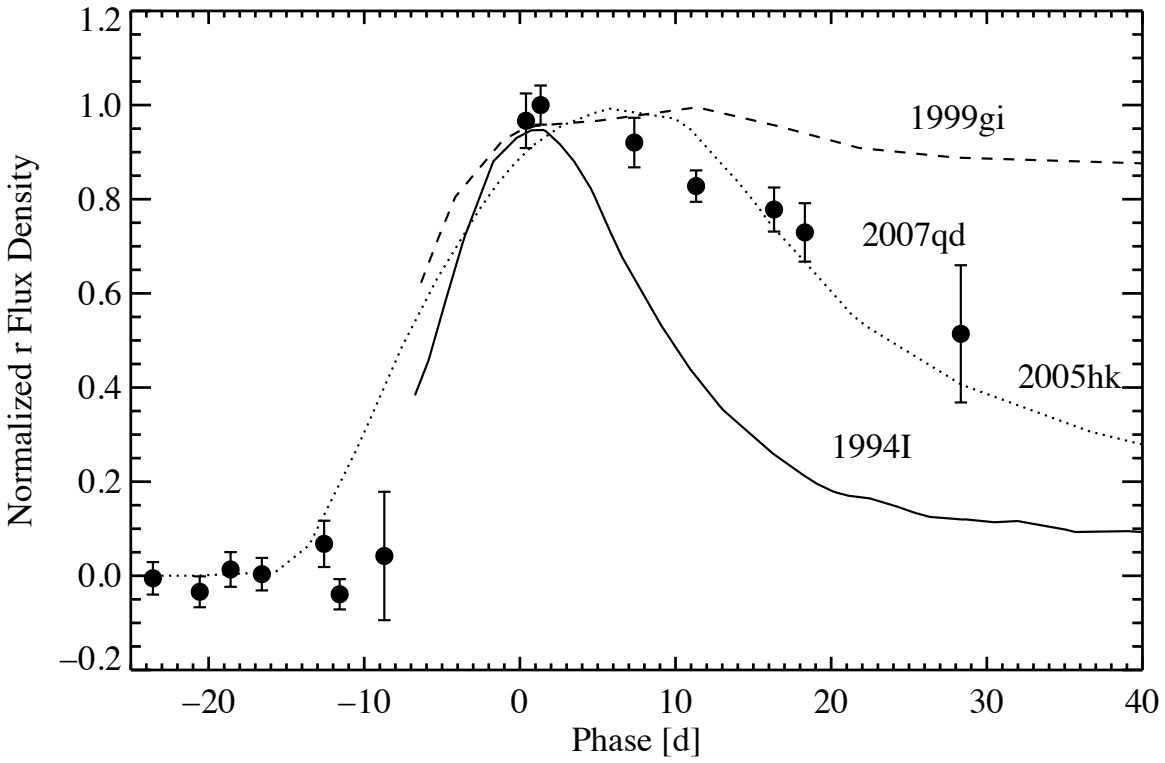

Fig. 3.— r-band light curves of 1994I (type Ic, solid line), 1999gi (type IIP, dashed line), 05hk (dotted line) and 07qd (data points) given in flux units. 1994I and 1999gi have been converted to the SDSS r bandpass via Fukugita et al. (1996) conversions utilizing V and R, and all fluxes have been normalized to each maximum. The time axis has also been corrected to 07qd's rest frame and each SN arbitrarily shifted in phase to best match the rise portion. 1994I, 1999gi and 05hk are shown without error bars for clarity and the interpolated segments were convoluted with a Gaussian FWHM of 2.

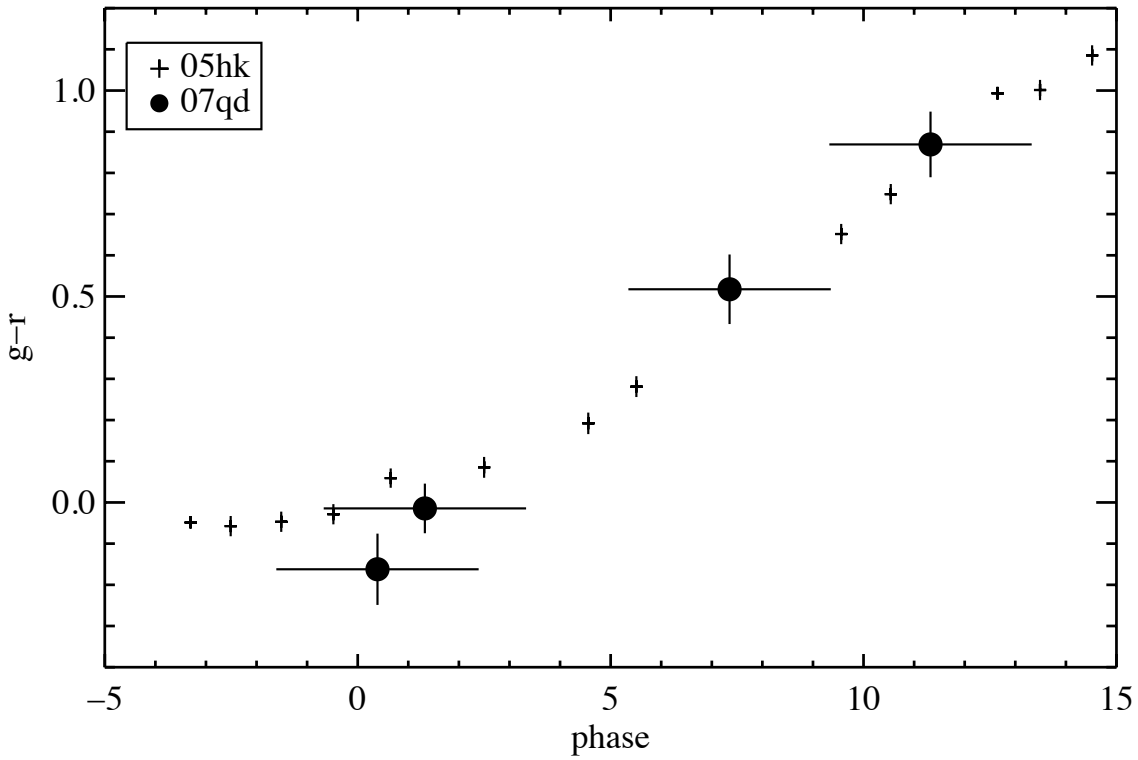

Fig. 4.— The $g-r$ color of 05hk and 07qd for the first two weeks past maxima is presented. The large error on 07qd's phase stems from the uncertainty in the time of maximum. Neither SN has been corrected for reddening.

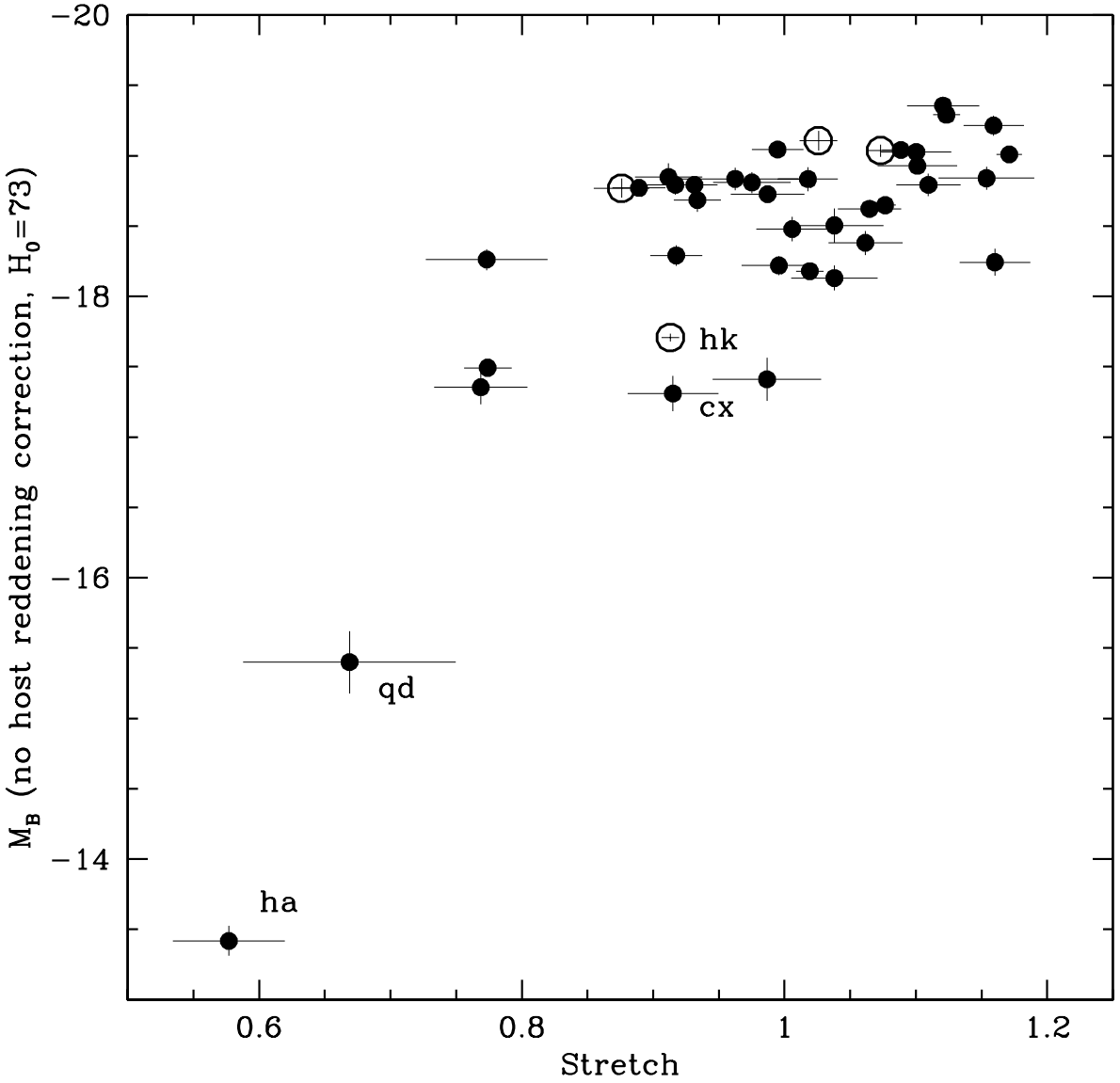

Fig. 5.— Light curve stretch factors are compared to the absolute magnitudes of peculiar SN Ia (open circles) along with SDSS II SN Ia with redshifts below 0.12 (Frieman et al. 2008; Sako et al. 2008). No correction for host extinction has been made. Peculiar SN have their names truncated for clarity.

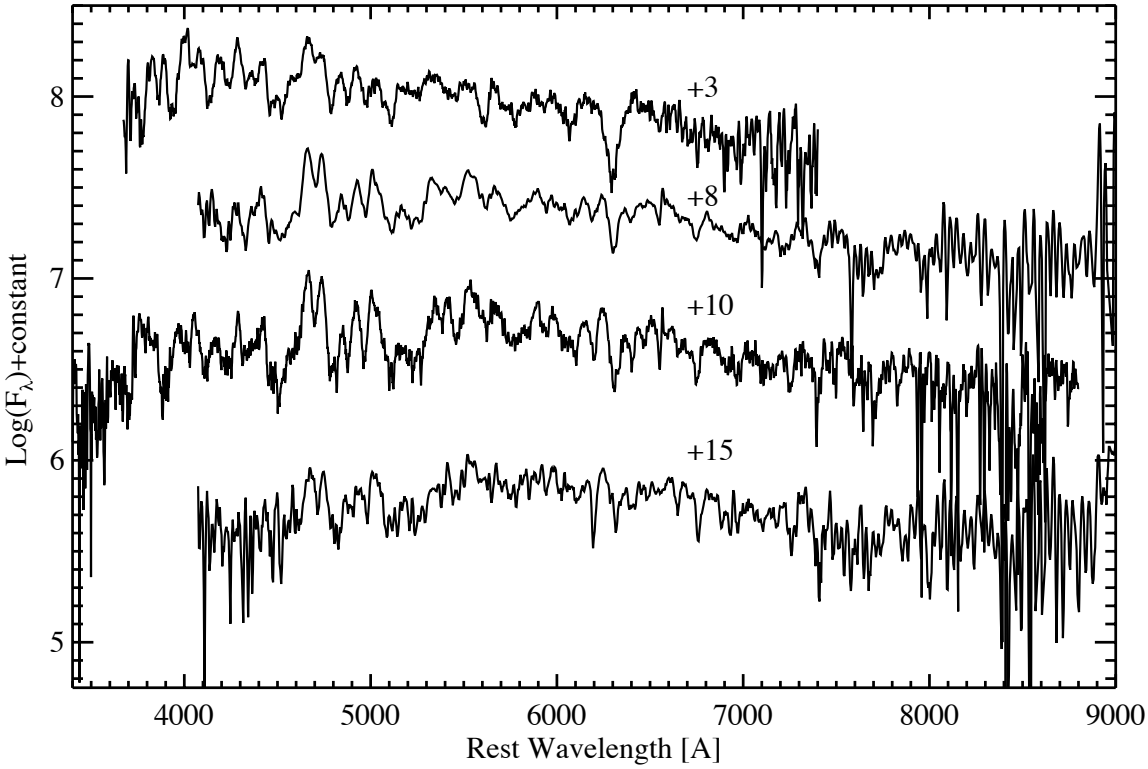

Fig. 6.— Time-evolution of 07qd's spectrum with a boxcar smoothing of 3 pixels in order to clearly show major velocity features. Times in this figure are given in days post B-maximum, atmospheric absorptions have been mitigated, and wavelengths have been Doppler corrected but not extinction corrected.

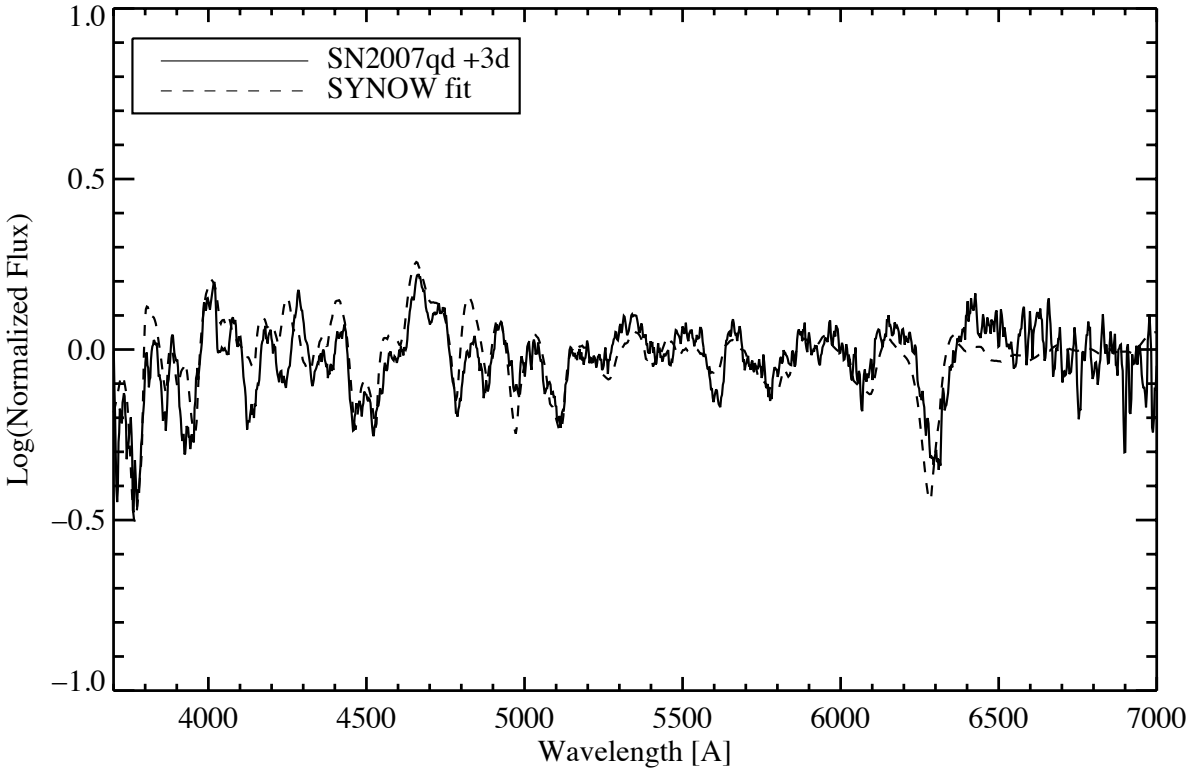

Fig. 7.— Spectrum for 07qd at 3 days past maximum and SYNOW fit. The flux has been normalized by a second-order Legendre Polynomial.

Table 4. SYNOW Parameters for figure 7[a,b]

Ion	τ	v_{min}	v_{max}	v_e	T_{exc}
Na I	0.3	4.5	8.0	4	10
Na I	0.5	2.8	4.5	1	10
Na I	0.1	8.0	10	2	10
Ca II	5.0	5.0	∞	1	10
V II	50	2.8	∞	1	10
S II	1.7	2.8	3.0	1	10
Si IV	2.0	2.8	∞	1	10
Si II	3.5	2.8	∞	1	10
F II	6.0	5.0	∞	1	10
K II	2.0	3.0	∞	1	10
Al I	6.0	2.8	∞	1	10
Fe III	1.0	2.8	∞	1	10
Fe II	2.0	2.8	∞	1	10
Co II	2.0	2.8	∞	1	10
C II	0.1	2.8	3.2	1	12
C III	0.5	2.8	8.0	2	10
C III	0.5	8.0	∞	2	10
O I	9.5	2.8	6.5	3	10
O III	1.8	2.8	∞	1	10

[a]Photospheric velocity of 2800 km s^{-1} and a black-body temperature of 10,000 K

[b]Velocities are given in units of 1000 km s^{-1} and T_{exc} values are given in units of 1000 K

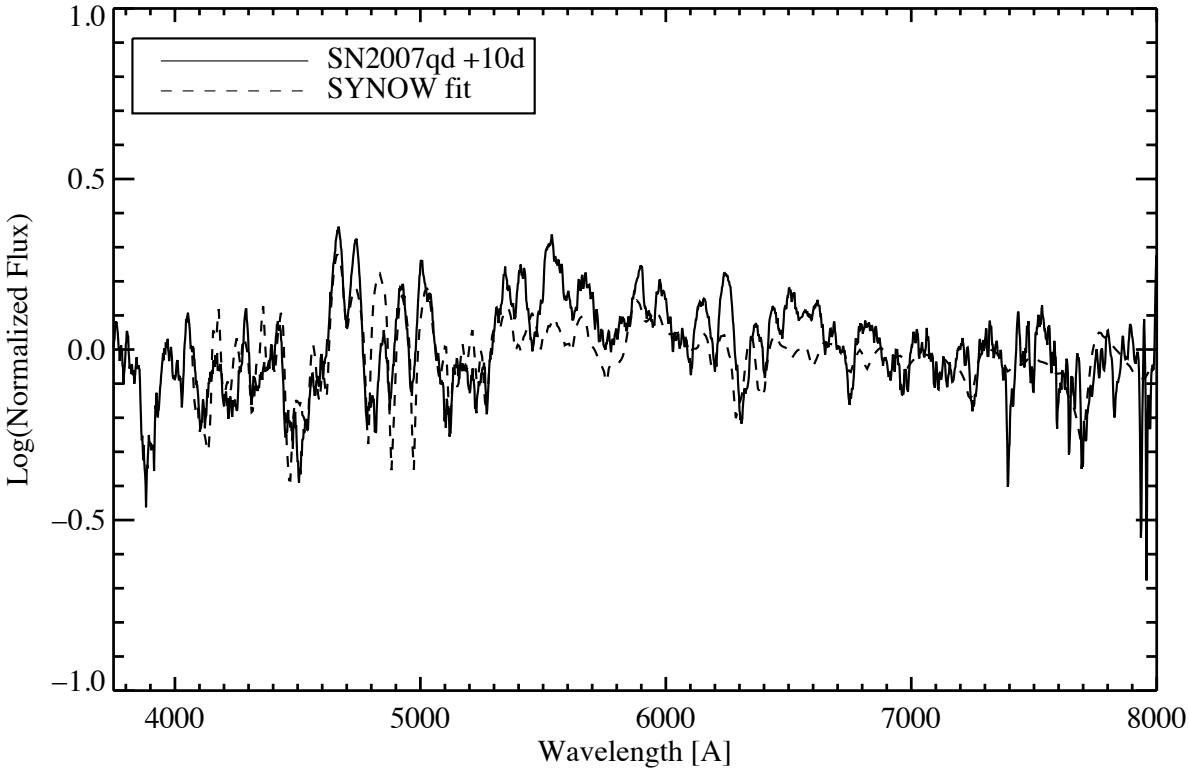

Fig. 8.— 07qd spectrum 10 days after maximum with SYNOW fit

Table 5. SYNOW Parameters for figure 8, at 10 days past maximum[a,b]

Ion	τ	v_{min}	v_{max}	v_e	T_{exc}
Co II	15	2.8	3.8	∞	5
Fe II	40	2.8	3.8	∞	8
Ca II	7.0	2.8	3.8	∞	3
Ca II	3.0	4.8	8.8	2	3
Na I	0.15	2.8	4.8	∞	5
Na I	0.15	4.8	8.8	2	5
Si II	3.0	2.8	3.8	∞	5
S II	4.0	2.8	3.0	∞	5
O II	.25	2.8	4.8	12	7
O I	.25	2.8	4.8	12	7

[a]Photospheric velocity of 2800 km s^{-1} and a black-body temperature of 8,000 K

[b]Velocities are given in units of 1000 km s^{-1} and T_{exc} values are given in units of 1000 K

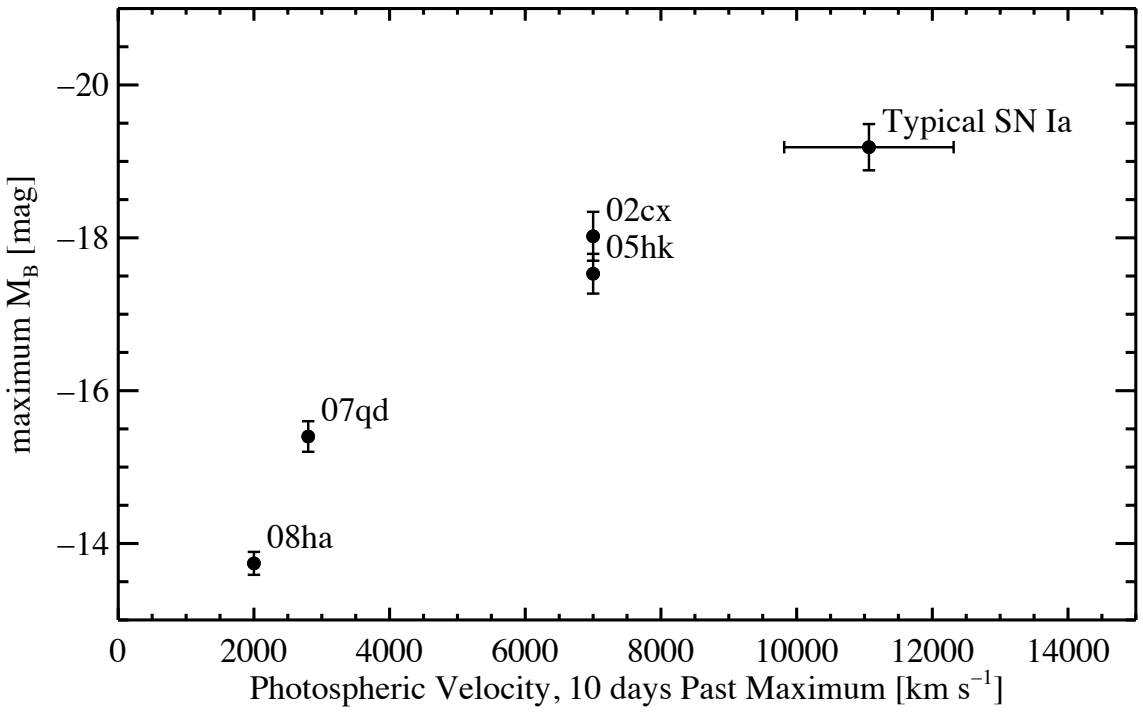

Fig. 9.— Estimated photospheric velocities at 10 days past maximum are rederenced by their maximum absolute madnitude. The "typical" point in the above right corner is the RMS magnitude and velocity of the normal SN Ia in Benetti et al. (2005).

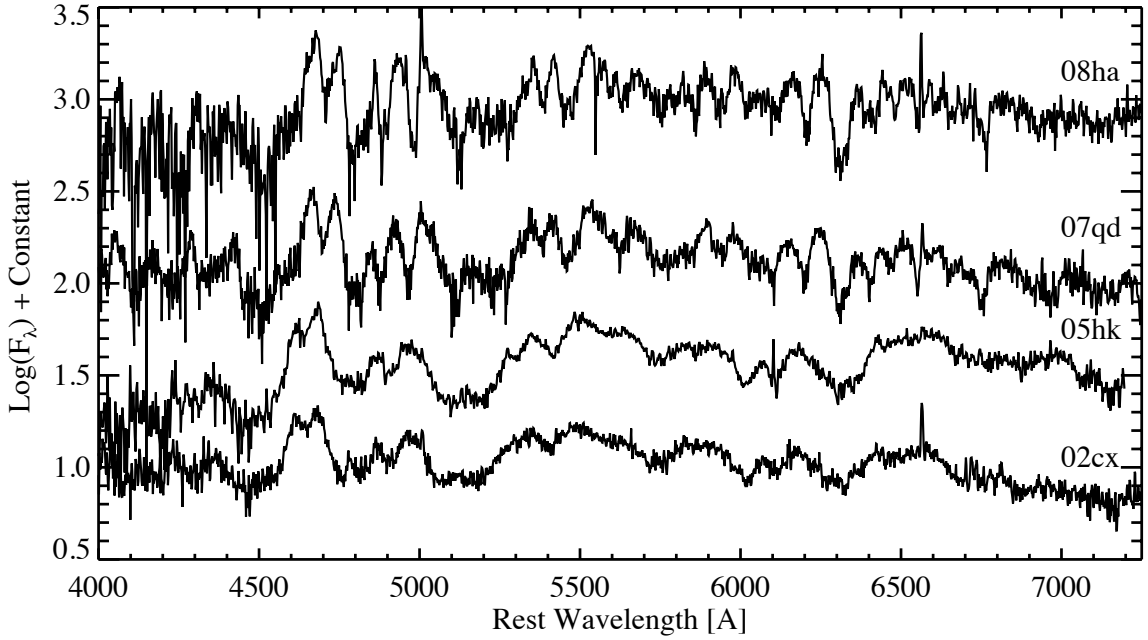

Fig. 10.— Comparison of 07qd's 10 day spectrum to that of 08ha (Foley et al. 2009), 05hk (Phillips et al. 2007) and 02cx (Branch et al. 2004) at similar epochs–10 days for 08ha and 12 days for both 05hk and 02cx. All spectra have been appropriately doppler corrected to their rest frames. Each feature of 07qd is redder than those of 05hk and 02cx indicating significantly slower photospheric velocities, while only slightly bluer than those of 08ha.

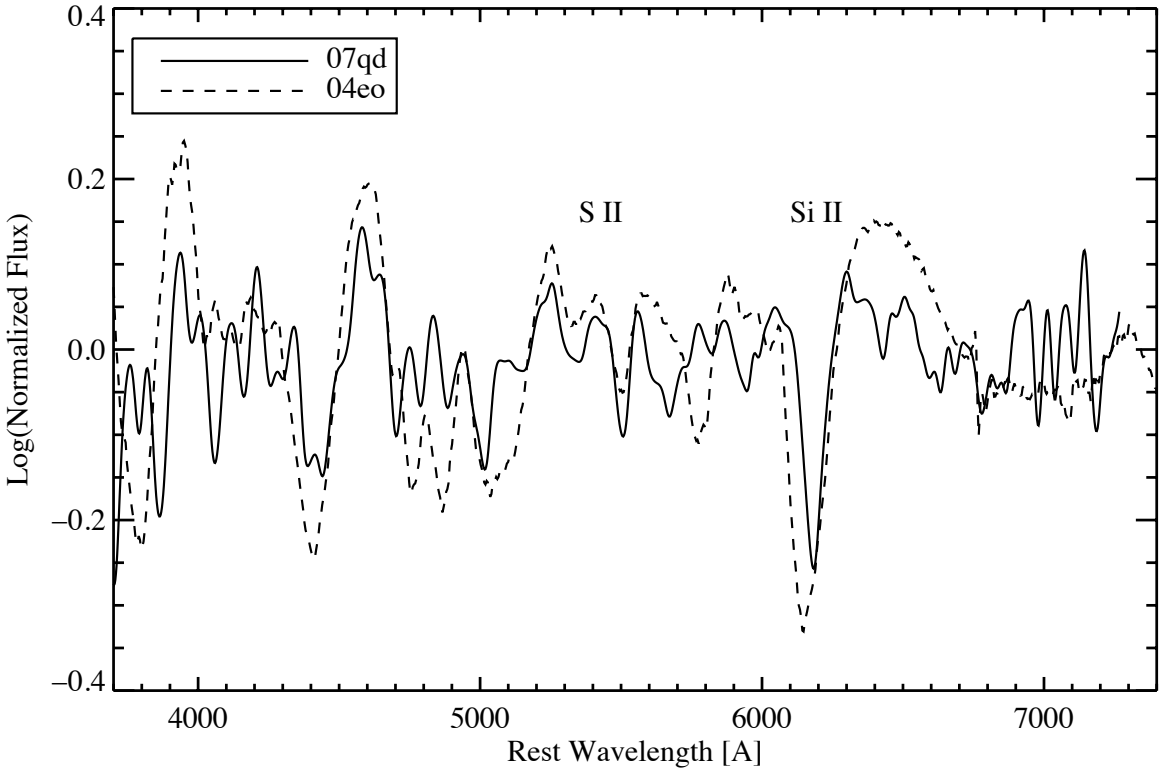

Fig. 11.— Spectrum of 07qd compared with that of SN Ia 2004eo (Pastorello et al. 2007) and shown in 2004eo's rest frame. The 3 day spectrum of 07qd has been convoluted with a Gaussian and blueshifted 5500 km s^{-1} to emphasize the similar Si II and S II features.